J. Plasma Fusion Res. SERIES, Vol. 2 (1999) 282–285

Magnetic Configuration Study of L = 1 Helical Axis Heliotron

YOKOYAMA Masayuki, ISAEV M.Yu.[1], NAKAMURA Yuji[2], WAKATANI Masahiro[2], SHAFRANOV V.D.[1] and COOPER W. Anthony[3]

National Institute for Fusion Science, Toki 509-5292, Japan

[1]Nuclear Fusion Institute, RRC "Kurchatov Institute", Moscow 123182, Russia

[2]Graduate School of Energy Science, Kyoto University, Uji 611-0011, Japan

[3]Centre de Recherches en Physique des Plasmas, EURATOM Ass. Confédération Suisse, Ecole Polytechnique Fédérale de Lausanne, Switzerland

(Received: 18 December 1998 / Accepted: 20 May 1999)

Abstract

The design studies of L = 1 helical axis heliotron have been progressed at Kyoto University. The experimental device based on this concept, Heliotron J, is designed to have the L = 1 continuous helical coil with two sets of toroidal coils and three pairs of poloidal coils for the experimental flexibility. In this paper, flexibility of helical axis heliotron configurations are described in relation with the poloidal coil current control.

Keywords:

helical axis heliotron, bumpy field, MHD equilibrium, Mercier stability, collisionless particle confinement, neoclassical transport

1. Introduction

The helical axis heliotron device, Heliotron J (H-J), has been proposed at Kyoto University to explore the advanced helical system [1]. Its major radius is R_0 = 1.2m and averaged magnetic field strength at the magnetic axis is 1.0–1.5T. Typical plasma minor radius is a = 0.1 – 0.2m. One of the main purposes is to do the basic experimental study of helical magnetic axis configuration. In order to keep the experimental flexibility and easy access, the $L = 1/M = 4$ continuous helical field coil (HFC) with pitch modulation $\alpha = -0.4$ has been chosen [2]. The winding law is defined as $\theta = \pi + (M/L)\phi - \alpha \sin(M/L)\phi$, where $L(M)$ is the pole (pitch) number and $\theta(\phi)$ denotes the geometrical poloidal (toroidal) angle. Negative pitch modulation is effective to form the vacuum magnetic well in the entire plasma region. In addition, recent studies have shown the significant roles of the bumpy field for improving the collisionless particle confinement [3] and controlling the bootstrap current [2]. The bumpy field is also the important component which was not present in planar axis heliotrons. There are also two sets of toroidal field coils (TFC-A,B) with different coil current. This current modulation is effective to control the bumpy field externally in a wide range. In addition, three pairs of poloidal field coils (PFC) have been proposed for further flexibility. The effects of TFC currents were already described in Ref. [4]. Therefore, in this paper, the effects of PFC currents on collisionless particle confinement, neoclassical transport, magneto-hydrodynamic (MHD) equilibrium and stability properties are described.

Corresponding author's e-mail: yokoyama@nifs.ac.jp

2. Magnetic Configuration Control through Poloidal Coils

One requirement for the coil design of H-J is that the set of PFC (PFC-OV) used in the Heliotron E [5] is usable to generate a uniform vertical field. In addition to PFC-OV, two sets of PFC have been considered. Here, the following parameters are fixed to emphasize the effects of PFC current control: (1) $B_t(1.2m)/B_h(1.2m) = 1.5$, where $B_t(1.2m)$ ($B_h(1.2m)$) is the toroidal field strength by TFC (HFC) at $R = 1.2$m, (2) $I_{TA}/I_{TB} = 5/2$, where $I_{TA}(I_{TB})$ is the current in TFC-A (TFC-B), (3) PFC-OV coil current is 0.84 MA in the opposite direction to HFC current with 0.96 MA. An example of two sets of PFC positions is $(R, Z) = (1.7, \pm 0.78)$m (Auxiliary Vertical, PFC-AV) and $(R, Z) = (0.45, 0)$m (Inner Vertical, PFC-IV). Here, it is noted that the PFC-IV is one coil for rough grasp of its roles, however; the possibility of division into two coils is not removed. Indeed, the present coil design of H-J has two coils of PFC-IV.

Figure 1 shows the effects of PFC-AV and PFC-IV currents (I_{AV} and I_{IV}) on principal magnetic configuration properties. Here, the horizontal axis denotes the I_{AV} (per one coil) and the vertical the I_{IV} with the definition that the current in the same direction as HFC is positive. The listed numbers are averaged plasma major radius ($\langle R_{ax}\rangle$m, $\iota(0)/\iota(a)$, vacuum magnetic well at plasma minor radius of 10 cm and $B_{10}(a)/(a/\langle R_{ax}\rangle)$ at vacuum case. Here B_{10} is the toroidicity of the magnetic field strength in the Boozer coordinates (s, θ_B, ζ_B) [6]. The B_{min} contours is also shown for each configuration, which is obtained by using only the dominant field spectra for simplicity. From Fig. 1, the following points are concluded. (1) As $\langle R_{ax}\rangle$ becomes larger, B_{min} contours tend to open. (2) The vacuum magnetic well becomes deeper and, in the same time, the ι becomes higher as I_{IV} becomes less negative. (3) The vacuum magnetic well can be maintained with positive I_{AV} even when $\langle R_{ax}\rangle$ becomes smaller (comparison between (I_{AV}, $I_{IV} = (0.0, 0.0)$ and $(0.0, 0.7)$ cases). (4) There is a possibility of varying the vacuum magnetic well depth with almost similar $\langle R_{ax}\rangle$, ι and B_{min} contours by varying I_{AV} and I_{IV} simultaneously (comparison between (I_{AV}, I_{IV}) = $(0.0, 0.0)$ and $(0.08, 1.0)$ cases). These imply the flexible magnetic configuration control with the poloidal coil current variation, which also contributes to the flexibility in H-J experiments.

3. Comparison of Magnetic Configuration Properties

In this section, principal plasma confinement properties are compared between several configurations shown in Fig. 1. Here, four configurations with different characteristics are considered.

201: (I_{AV}, I_{IV}) = $(0.0, 0.0)$, $\langle R_{ax}\rangle \sim R_0$.
203: (I_{AV}, I_{IV}) = $(0.0, 0.7)$, $\langle R_{ax}\rangle < R_0$, high $B_{10}/(a/\langle R_{ax}\rangle)$, keeping the magnetic well even when $\langle R_{ax}\rangle < R_0$.
207: (I_{AV}, I_{IV}) = $(0.0, -1.0)$, $\langle R_{ax}\rangle > R_0$, $B_{10}/(a/\langle R_{ax}\rangle) \sim 1$, unclosed B_{min} contours.
212: (I_{AV}, I_{IV}) = $(0.16, 1.0)$, $\langle R_{ax}\rangle > R_0$, unclosed B_{min} contours, deeper magnetic well, higher ι.

The ratios, B_{10}/B_{11} and B_{01}/B_{11} (at $r/a = 0.5$), are summarized in Table I. Here, B_{11} and B_{01} denote the principal helicity and bumpiness, respectively. The importance of negative B_{01}/B_{11} for improving the particle confinement has been clarified in Ref. [2]. This ratio becomes more negative as $\langle R_{ax}\rangle$ is reduced with more positive I_{IV}. Based on this favorable ratio of B_{01}/B_{11}, B_{min} contours tend to close for this region of I_{IV}. However, when I_{AV} is set to be positive, $\langle R_{ax}\rangle$ becomes larger and B_{min} contours become open (cf., comparison

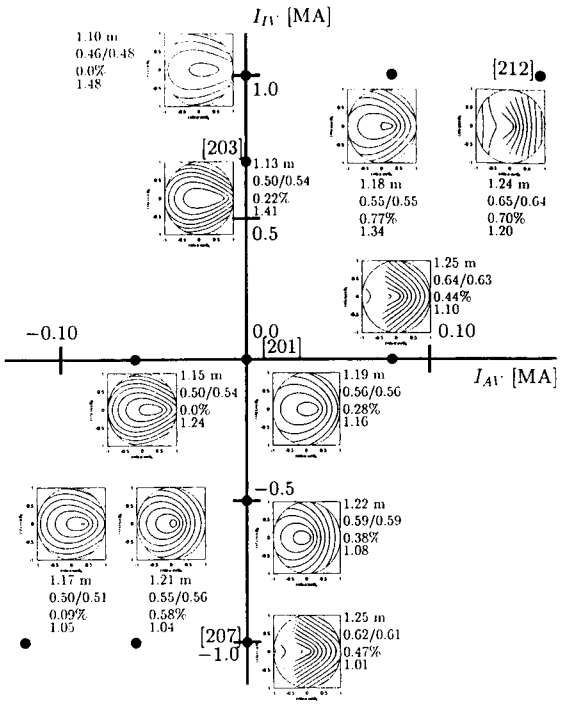

Fig. 1 Relations between magnetic configuration properties and (I_{AV}, I_{IV}).

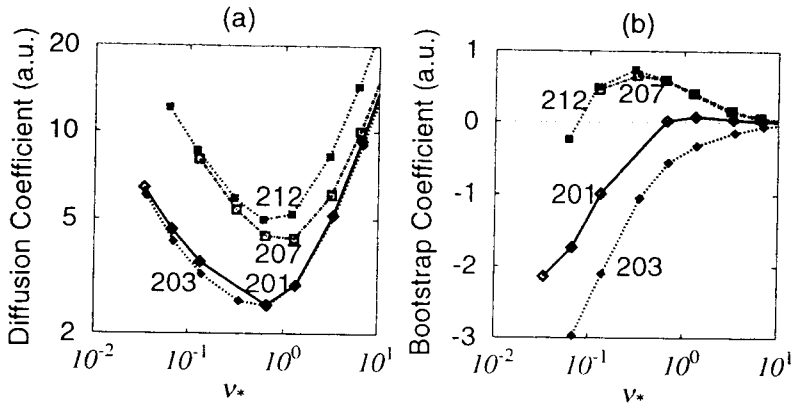

Fig. 2 (a) Neoclassical particle diffusivity and (b) bootstrap coefficient for configurations 201, 203, 207 and 212.

Table I The ratios, B_{10}/B_{11} and B_{01}/B_{11}, for configurations 201, 203, 207 and 212.

Configuration	B_{10}/B_{11}	B_{01}/B_{11}
201	0.75	–0.65
203	0.88	–1.13
207	0.66	0.08
212	0.76	0.17

between 203 and 212). In this case, active control of bumpy field using TFC (increasing the ratio, I_{TA}/I_{TB}) would be required for closing B_{min} contours.

Collisionless particle confinement is studied with the guiding center equations in the Boozer coordinates [7]. The protons are launched from $r/a = 0.25, 0.5, 0.75$ magnetic surfaces with assumed temperature profile: $T(r) = 1.0[1 - (r/a)^2]$. The number of launched particles from uniformly distributed points in the Boozer poloidal and toroidal angles is defined by considering the area element. The particles are followed for 2 ms or until they cross the plasma boundary. The loss rate for configurations 201 and 207 is 12.6% and 24.2%. The collisionless particle confinement improves as B_{01}/B_{11} becomes almost zero to negative, reflecting the closure of B_{min} contours.

The DKES code [8] has been utilized to evaluate the neoclassical transport properties. They are calculated at the magnetic surface with $|B_{10}| = 0.1$. Therefore, the contribution from axisymmetric part of the magnetic field can be considered to be equal except the difference of ι. Figure 2(a) shows the monoenergetic particle diffusion coefficient and 2(b) the bootstrap coefficient, where ν_* denotes the effective collision frequency. The $1/\nu$ diffusivity reduces for configurations 201 and 203

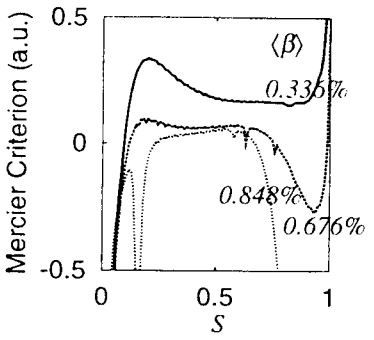

Fig. 3 Mercier stability criterion for several $\langle\beta\rangle$ values for the configuration 212.

with negative B_{01}/B_{11} compared to that for 207 and 212 with positive or almost zero B_{01}/B_{11}. The bootstrap coefficient also changes with B_{01}/B_{11}. The B_{10}/B_{11}, which is the one of the key parameters to reduce the bootstrap current in the Wendelstein 7-X (W7-X) [9], does not vary in a wide range as listed in Table I. Therefore, it is considered that the variation of bootstrap coefficient is mainly due to the bumpy field. Figures 2 imply flexibility in experiments for neoclassical transport properties in H-J through PFC current variation.

The MHD equilibrium has been calculated by the VMEC [10] with a rather broad pressure profile, $P(s) = P(0)(1 - s^2)^2$, and currentless condition. Based on the MHD equilibrium, ideal Mercier criterion (D_M) [11] has been evaluated by the TERPSCICHORE code [12]. As an example, the results for the configuration 212 (the deepest magnetic well among four configurations) is shown in Fig. 3, where the positive D_M corresponds to the Mercier stability. From this figure, it is concluded

that the configuration 212 is Mercier stable up to $\langle\beta\rangle \sim 0.5\%$. The spike-like behavior at $\langle\beta\rangle = 0.848\%$ corresponds to the rational surface with $\iota = 4/6$. It arises from the resonant parallel current in the vicinity of a rational surface, which is obtained by solving the magneto-differential equation derived from the local equilibrium equation ("indirect method"). The narrow spike can be considered to be physically remedied by the flattening of the pressure profile in the magnetic island region. This has been numerically justified in Ref. [13] for the LHD by the "filtering" of the resonant contribution to Mercier criterion, which reproduces the result based on the VMEC equilibrium quantities ("direct method"). However, it is pointed out there that the discrepancy between indirect and direct method become remarkable around the region where the ι has a local minimum (and low shear). Therefore, to determine the ideal Mercier stability limit in detail in the H-J with low shear, careful comparisons between indirect and direct methods should be accomplished. By the way, D_M becomes negative in rather wide region even when $\langle\beta\rangle < 0.5\%$ due to the presence of two points of $\iota = 4/8$ by the change of ι in other three configurations. From this point of view, the configuration 212 with higher ι is considered to have a wider margin for the appearance of $\iota = 4/8$. Therefore, the reduction of Pfirsch-Schlüter current (or reduction of Shafranov shift) should be pursued to keep ι unchanged and/or to avoid the dangereous low-order rational surfaces.

4. Summary

The flexibility of helical axis heliotrons based on poloidal coil current control is presented. The ratios, toroidicity/helicity and bumpiness/helicity in the magnetic field can be widely controlled, which varies the collisionless particle confinement and bootstrap current. The vacuum magnetic well is also varied to maintain the Mercier stability, however; the possibility of low-order rational surface at finite beta cases due to the ι change may cause the Mercier unstable region. The shear generation with Ohmic current would be one of the possibilities for avoiding this unstable region. Further detailed study for maintaining the MHD stability at higher beta values should be explored.

References

[1] F. Sano *et al.*, J. Plasma Fusion Res. SERIES **1**, 168 (1998).
[2] M. Yokoyama, Y. Nakamura and M. Wakatani, J. Plasma Fusion Res. **73**, 723 (1997).
[3] M. Yokoyama, N. Nakajima, M. Okamoto *et al.*, J. Plasma Fusion Res. SERIES **1**, 445 (1997).
[4] M. Wakatani, Y. Nakamura *et al.*, *Plasma Physics and Controlled Nuclear Fusion Research 1998*, in press.
[5] K. Uo *et al.*, *Plasma Physics and Controlled Nuclear Fusion Research 1980* (Proc. 8th Int. Conf. Brussels, 1980), Vol.1, IAEA, Vienna, 217 (1981).
[6] A.H. Boozer, Phys. Fluids **23**, 904 (1980).
[7] R. Fowler *et al.*, Phys. Fluids **28**, 338 (1985).
[8] S.P. Hirshman *et al.*, Phys. Fluids **29**, 2951 (1986).
[9] G. Grieger *et al.*, Phys. Fluids **B4**, 2081 (1992).
[10] S.P. Hirshman *et al.*, Comput. Phys. Commun. **43**, 143 (1986).
[11] C. Mercier, Nucl. Fusion **1**, 47 (1960).
[12] W.A. Cooper, Plasma Phys. and Contr. Fusion, **34**, 1011 (1992).
[13] K. Ichiguchi, Nucl. Fusion, **36**, 1157 (1996).